AJNR

Fibrosing inflammatory pseudotumors involving the skull base: MR and CT manifestations with histopathologic comparison.

M H Han, J G Chi, M S Kim, K H Chang, K H Kim, K M Yeon and M C Han

AJNR Am J Neuroradiol 1996, 17 (3) 515-521
http://www.ajnr.org/content/17/3/515

Fibrosing Inflammatory Pseudotumors Involving the Skull Base: MR and CT Manifestations with Histopathologic Comparison

Moon Hee Han, Je G. Chi, Myung Soon Kim, Kee Hyun Chang, Kwang Hyun Kim, Kyung Mo Yeon, and Man Chung Han

PURPOSE: To describe the MR and CT features of fibrosing inflammatory pseudotumors of the skull base region, and to document the MR signal intensity of the lesions with histopathologic comparison. **METHODS:** We reviewed the MR and CT studies of five patients with pathologically proved fibrosing inflammatory pseudotumor involving the skull base. Unenhanced spin-echo T1- and T2-weighted and contrast-enhanced T1-weighted MR images were obtained at 0.5 T in three patients and at 1.5 T in two patients. MR findings were correlated with histopathologic findings in all five cases, and the enhancement pattern was compared with CT findings in three cases. **RESULTS:** In three cases, the cavernous sinus was involved unilaterally, with adjacent extracranial infiltrative masses. In one case, both orbits, the cavernous sinuses, and the tentorium were involved with diffuse infiltrative lesions. One patient had an infiltrative nasopharyngeal mass; and in all five patients, MR images showed localized involvement of the skull base, with bone marrow replaced by tumor. The soft-tissue lesions were hypointense on T2-weighted images in all five cases and showed homogeneous contrast enhancement. Histopathologic studies revealed scanty inflammatory cell infiltration with densely fibrotic background in all cases. The hypointensity of the lesions on T2-weighted images seemed to be related to the degree of fibrosis. **CONCLUSION:** Fibrosing inflammatory pseudotumor shows characteristic MR findings of infiltrative lesion with bone destruction and hypointensity on T2-weighted images. The lack of mobile protons due to the fibrotic background and/or high cellularity of the lesions may be the reason for their hypointensity and weaker enhancement on MR images.

Index terms: Skull, base; Skull, neoplasms; Head, inflammation

AJNR Am J Neuroradiol 17:515–521, March 1996

Inflammatory pseudotumors of the head and neck are idiopathic, inflammatory lesions that most commonly involve the orbit (1, 2). They include a diverse group of lesions characterized by inflammatory cell infiltration and variable fibrotic responses. In addition to the orbit, other areas of involvement include the larynx, the paranasal sinuses, and the soft tissues of the neck and esophagus (3–6). Similar lesions have been described in other areas, such as the lungs (7).

Inflammatory pseudotumor involving the skull base is rare. The purpose of this article is to describe the magnetic resonance (MR) and computed tomographic (CT) features of five cases of pathologically proved fibrosing inflammatory pseudotumor involving the skull base and to compare the MR signal intensities of the lesions with histopathologic findings.

Materials and Methods

We reviewed the MR and CT studies of five patients with pathologically proved fibrosing inflammatory pseudotumor involving the area of the central skull base. Clinical and radiologic features of the patients are summarized in the Table. All five patients had long-standing (4 months to

Received April 5, 1995; accepted after revision September 26.

Presented at the annual meeting of American Society of Neuroradiology, Nashville, Tenn, May 1994.

Supported by grant no. 02–94–189 from the Seoul National University Hospital Research Fund.

From the Departments of Diagnostic Radiology (M.H.H., K.H.C., K.M.Y., M.C.H.), Pathology (J.G.C.), and Otolaryngology (K.H.K.), Seoul (Korea) National University College of Medicine; and the Department of Diagnostic Radiology, Wonju (Korea) Medical College (M.S.K.).

Address reprint requests to Moon Hee Han, MD, Department of Diagnostic Radiology, Seoul National University Hospital, 28 Yeongun-dong, Chongro-ku, Seoul 110–744, Korea.

AJNR 17:515–521, Mar 1996 0195-6108/96/1703–0515

Clinical and radiologic findings in five patients with fibrosing inflammatory pseudotumors of the skull base

Case	Age, y/ Sex	Signs and Symptoms	Imaging Studies	Region of Tumor	Involvement		Degree of Signal Intensity on MR Images			Histopathologic Findings	
					Bone	Dura	T1-Weighted	T2-Weighted	Contrast Enhanced	Fibrosis	Cellularity
1	38/M	Ophthalmoplegia	MR (0.5 T), CT	CS, ITF	Sphenoid	MCF	Iso	Sl hypo	+	+	++
2	30/M	Facial nerve palsy	MR (1.5 T), CT	Nasopharynx	Clivus	MCF	Iso	Sl hypo	++	++	++
3	36/M	Ophthalmoplegia	MR (0.5 T), CT	CS, ITF, orbit	Clivus	Tentorium	Sl hypo	Mk hypo	++	+++	+
4	57/M	Trigeminal neuralgia	MR (0.5 T)	CS, ITF, brain	Sphenoid	MCF	Sl hypo	Mk hypo	++	+	+++
5	25/M	Hearing loss	MR (1.5 T)	CS, ITF	Sphenoid	MCF, PC	Mk hypo	Mk hypo	+	+	++

Note.—CS indicates cavernous sinus; ITF, infratemporal fossa; MCF, middle cranial fossa; PC, petroclival; iso, isointensity; sl hypo, slight hypointensity; mk hypo, marked hypointensity; +, mild; ++, moderate; and +++, severe.

2 years) signs and symptoms of various cranial nerve dysfunction. No patient had a history of craniofacial surgery or specific infection; and none had diabetes mellitus at the time of diagnosis. Patients with histopathologic findings of prominent plasma cell infiltration that were diagnosed as plasma cell granulomas were excluded from the study.

All five patients were examined with MR imaging at 1.5 T (two cases; Magnetom 1.5, Siemens, Germany, and GE Signa, General Electric, Milwaukee, Wis) or at 0.5 T (three cases; Supertech-5000, GoldStar, Korea, and Gyroscan, Philips, the Netherlands). Spin-echo T1-weighted 500/12–30/4 (repetition time [TR]/echo time [TE]/excitations) and long-TR/short- and long-TE (2500–3000/30, 90/2) images were obtained. Contrast-enhanced T1-weighted images in axial and coronal planes were obtained after intravenous injection of gadopentetate dimeglumine (0.1 mmol/kg; Magnevist, Schering, Germany) in all cases.

Three of five patients were also examined with CT (GE 9800, General Electric). Contrast-enhanced axial and coronal scans were obtained with 3- to 5-mm section thickness.

MR findings—including intracranial changes in signal intensity of the lesions and bone—were described, and enhancement patterns were compared with CT findings in three cases. The degree of fibrosis and the extent of inflammatory cell infiltration were evaluated and were graded relative to findings at histopathologic examination, and these findings were then compared with MR signal intensity patterns in all cases.

Results

In four of the five patients studied (cases 1, 3, 4, and 5), the muscles of mastication were involved unilaterally by infiltrative mass lesions (Fig 1). In three patients (cases 1, 4, and 5), the cavernous sinus was involved unilaterally with adjacent extracranial infiltrative masses. In one patient (case 3), both orbits, the cavernous sinuses, and the edges of the tentorium of cerebellum were involved with diffuse and symmetric infiltrative lesions (Fig 2). One patient (case 2) had an infiltrative nasopharyngeal mass involving the stylomastoid foramen (Fig 3).

In all five cases, localized involvement of the skull base was seen on MR images where tumor replaced the signal of the fatty bone marrow; in two of these, the bone lesions were also seen on CT scans. The greater wing of the sphenoid bone was involved unilaterally in three patients (cases 1, 4, and 5; Fig 1), and the clivus was involved in two patients (cases 2 and 3; Figs 2 and 3). One patient (case 2) also had unilateral involvement of the mastoid bone (Fig 3).

The soft-tissue mass lesions were hypointense relative to brain on both T1- and T2-weighted images in three patients (cases 3, 4, and 5; Figs 1 and 2). In two patients (cases 1 and 2), the lesions were isointense with brain on T1-weighted images and hypointense relative to brain on T2-weighted images (Fig 3). In all cases, the lesions of the soft tissues and bones showed homogeneous enhancement on MR images after injection of contrast material. In one patient with lesions of both orbits (case 3), contrast-enhanced CT scans showed greater enhancement of the retrobulbar soft-tissue lesions than did the MR images, which showed slight enhancement (Fig 2).

Thickening and enhancement of the intracranial dural structures adjacent to the lesions were seen on contrast-enhanced MR images in all patients. In four patients (cases 1, 2, 4, and 5), dural involvement was seen in the unilateral middle cranial fossa, and the tentorium was involved in one patient (case 3). In one patient

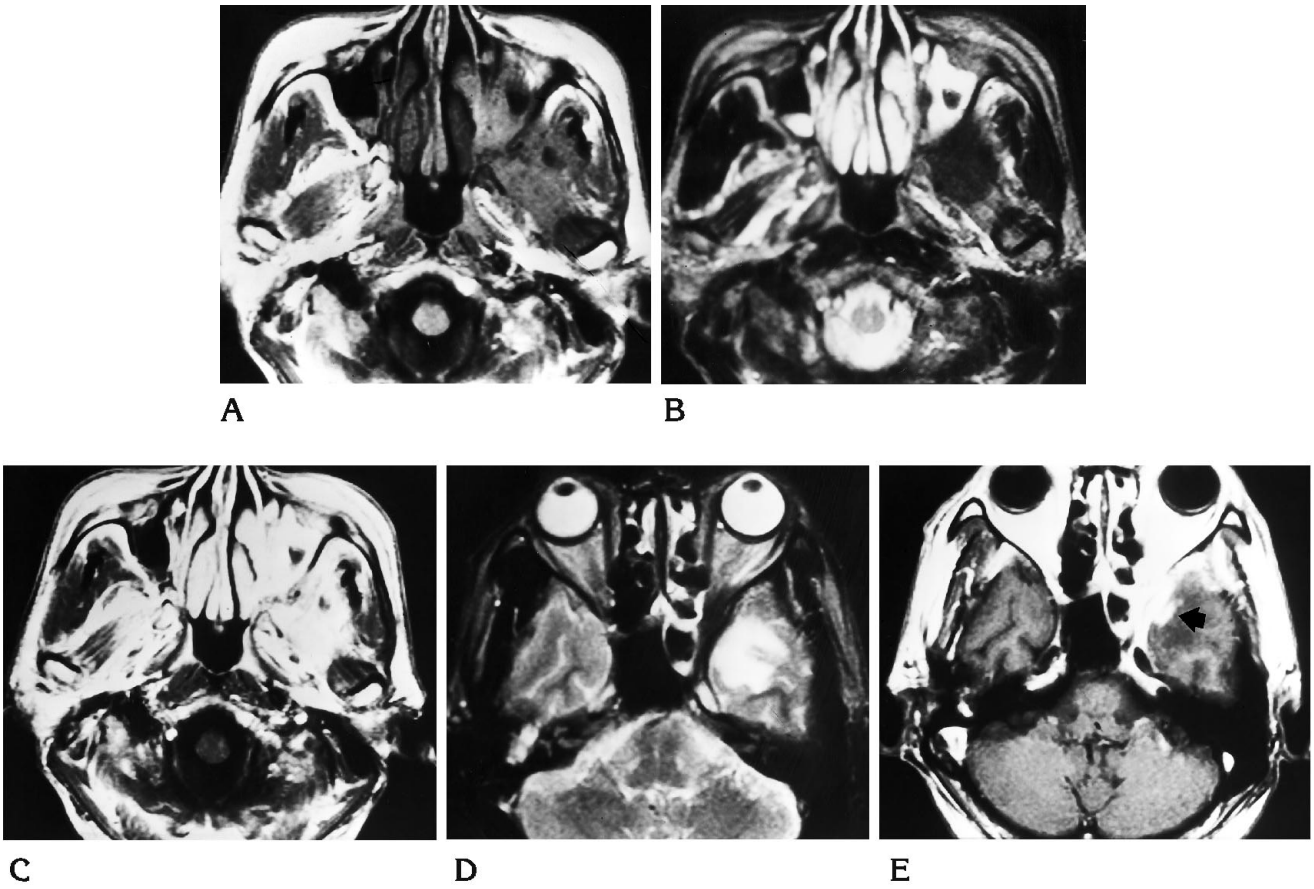

Fig 1. Case 4: 57-year-old man with trigeminal neuralgia.

A, T1-weighted (500/20) axial MR image at the level of the maxillary sinus shows a poorly defined infiltrative lesion with intermediate intensity in the left infratemporal fossa. Fat planes of the left pterygopalatine fossa and the planes of the muscles of mastication are obliterated. Posterior wall of the left maxillary sinus is also involved with obliteration of the retromaxillary fat pad.

B, T2-weighted (3000/90) axial MR image shows very low signal intensity of the left infratemporal fossa lesion. The lesion within the left maxillary sinus has very high signal intensity, suggesting inflammatory mucosal thickening.

C, Contrast-enhanced T1-weighted axial MR image at the same level as *A* shows diffuse and strong enhancement of the left infratemporal fossa lesion. Posterior wall of the left maxillary sinus, pterygopalatine fossa, and pterygoid plates are also enhanced.

D, T2-weighted axial MR image at the level of the midorbit shows a localized hyperintense lesion in the medial left temporal lobe of the brain.

E, Contrast-enhanced T1-weighted axial MR image at the same level as *D* shows diffuse dural enhancement of anteromedial aspect of the left middle cranial fossa with a focal nodular enhancement in the left temporal cortex (*arrow*). An area of hypointensity is seen in surrounding parenchyma of the left temporal lobe.

(case 4), localized brain swelling, hyperintensity on T2-weighted images, and focal cortical enhancement were seen in the adjacent anterior temporal lobe (Fig 1).

Histopathologic specimens were obtained in all patients by open surgical biopsy of the soft-tissue mass lesions. Histopathologic examinations revealed lymphocyte and plasma cell infiltration and densely fibrotic changes with collagen deposition and fibroblastic activity in all cases (Figs 2E and 3G). The extent of collagen deposition, fibroblastic activity, and inflammatory cell infiltration of the lesions was variable. The degree of fibrotic changes of the lesions seemed to vary inversely with the inflammatory cell infiltration. Signal intensity of the lesions was not closely related to the degree of fibrosis or cellularity found on histopathologic specimens (Table). In one patient, in whom slight enhancement of the lesion was seen on MR images (case 2), prominent fibrosis and scanty inflammatory cell infiltration were apparent at microscopic examination (Fig 2E).

Microbiological studies were done during surgery or biopsy in all patients, but no specific microorganism was isolated. Similarly, no pa-

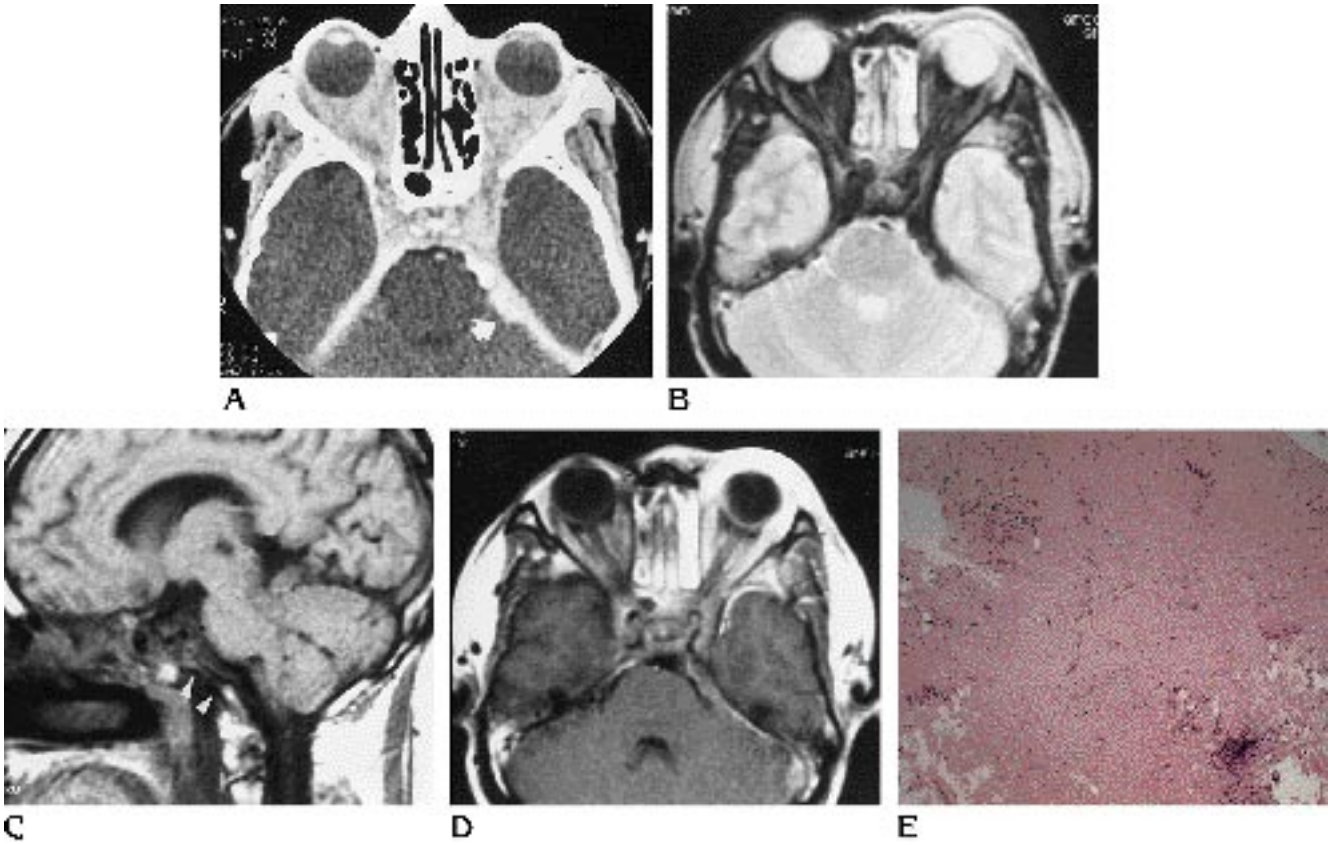

Fig 2. Case 3: 36-year-old man with a 4-month history of ophthalmoplegia.

A, Contrast-enhanced CT scan at the level of the midorbit shows total obliteration of the bilateral retrobulbar fat spaces, which are replaced by homogeneously enhancing lesion. Bilateral cavernous sinuses are involved by the lesion, and the edges of the tentorium of cerebellum are thickened and enhanced with mild irregularity in the left posterior aspect (*arrow*).

B, T2-weighted (2500/100) axial MR image shows diffuse hypointensity of the orbital and cavernous sinus lesions.

C, T1-weighted (500/30) sagittal image at the left cavernous sinus plane shows the clivus replaced by hypointense lesion (*arrowheads*).

D, Contrast-enhanced T1-weighted axial image at the same level as *B* shows slight enhancement of the orbital, cavernous sinus, and tentorial lesions. The degree of lesion enhancement appears weaker than that shown by CT, especially on the right side.

E, Histopathologic section shows scanty inflammatory cell infiltration with dense collagen deposition, suggesting severe fibrosis (hematoxylin-eosin stain, magnification ×100).

tient had evidence of fungal infection at microscopic examination.

After pathologic diagnosis, the patients were treated with extended steroid therapy for more than a month without any objective improvement or progression of cranial nerve dysfunctions. In one patient (case 3), a follow-up CT scan was obtained after 6 months of steroid therapy and showed no change in the extent of the lesion.

Discussion

Inflammatory pseudotumor of the head and neck is most often encountered as a benign, chronic, inflammatory lesion of the orbit with no known origin. Although some investigators have proposed a relationship between adjacent sinus inflammation and the occurrence of pseudotumor (8), findings in at least one large series have failed to document this association (9). The existence of many synonyms for *inflammatory pseudotumor* and the varied histopathologic findings of this process suggest that this is not a single disease entity but rather an umbrella term for any nonspecific chronic inflammatory mass lesion (10). So a disease with similar histopathologic findings of inflammatory pseudotumor located in a different site is thought to be a different disease with a different clinical course.

In some cases of inflammatory pseudotumor, temporal progression from acute inflammatory infiltration to chronic fibrosing process has been

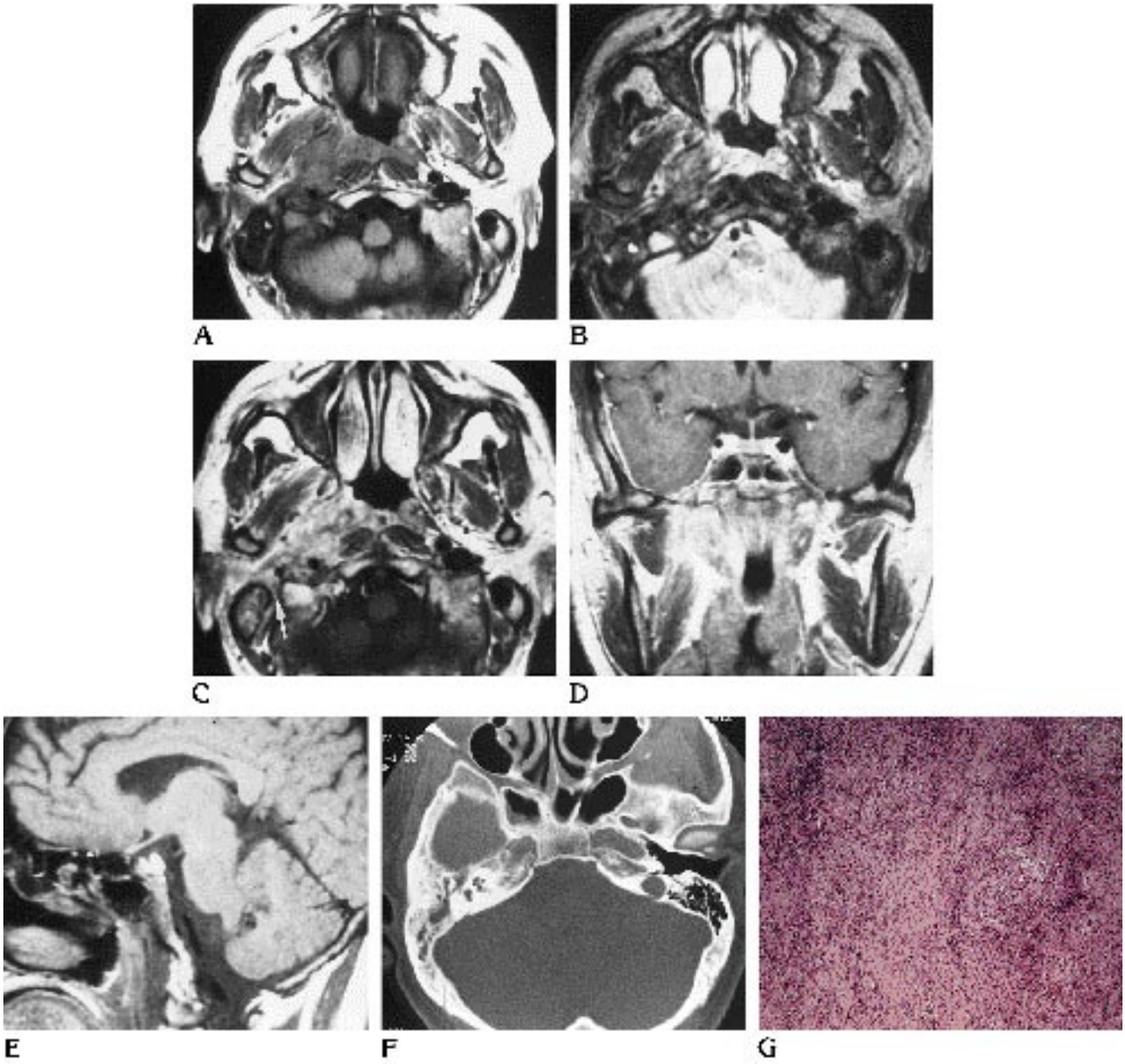

Fig 3. Case 2: 30-year-old man with 1-year history of facial palsy.

A, T1-weighted (500/20) axial MR image at the level of the nasopharynx shows a poorly defined mass with intermediate intensity in the right nasopharynx. Right parapharyngeal fat is partially obliterated. Note decreased signal intensity of the right mastoid process and adjacent occipital bone.

B, T2-weighted (3000/90) axial MR image shows hypointensity of the right nasopharyngeal lesion.

C, Contrast-enhanced T1-weighted axial MR image shows diffuse enhancement of the lesion. The right internal carotid artery is encased by the enhancing lesion and the right stylomastoid foramen is also enhanced (*arrow*). Right mastoid process and adjacent occipital bone are enhanced as compared with unenhanced image (*A*).

D, Contrast-enhanced T1-weighted coronal MR image shows diffuse enhancement of the right nasopharyngeal lesion and the dural surface of the right middle cranial fossa.

E, Unenhanced T1-weighted sagittal MR image shows localized replacement of the clival bone marrow with adjacent nasopharyngeal lesion.

F, Axial CT scan with bone window setting shows no significant abnormality in trabecular pattern of the clivus.

G, Histopathologic section shows diffuse inflammatory cell infiltration with a background of fibroblastic activity. Collagen deposition in this case seems to be less than that of case 3 (Fig 2) and cellularity of the lesion seems much higher (hematoxylin-eosin stain, magnification $\times 100$).

observed (2, 11, 12). The histopathologic findings in our patients may reflect a change from inflammatory to chronic pseudotumor, and their long histories of signs and symptoms may support this chronicity. However, we found no relationship between the duration of signs and symptoms and the degree of fibrosis in our series.

In most cases of orbital pseudotumor, the lesion is confined to the orbit without invasion of the bony walls (13). But in several reported cases of inflammatory pseudotumor of the maxillary sinus or infratemporal fossa, CT scans showed localized bone destruction (3, 4, 14, 15). In cases in which there is bone destruction, the distinction between pseudotumor and malignant neoplasm is very difficult without biopsy.

In all our cases, MR images showed extracranial soft-tissue lesions infiltrating the skull base with intracranial dural involvement. In general, these MR findings are strongly suggestive of malignant tumor. CT findings of enlarged muscles with preserved fascial planes between them has been reported as a suggestive finding of inflammatory-type lesions (5). In our series, however, fat planes within involved areas were obliterated, and this finding was not helpful for the differential diagnosis (Fig 1). The skull base changes seen in our cases cannot be distinguished from those of malignant bone invasion, and malignant tumor must be included in the differential diagnosis of lesions of the central skull base.

Changes of adjacent brain parenchyma with localized enhancement and surrounding edema were shown on MR images in one patient (case 4) in our series. This is also a finding suggestive of an aggressive lesion, and may be a reactive change to an adjacent dural lesion or to direct parenchymal invasion. In this case, the diagnosis was confirmed by results of an open biopsy of the infratemporal fossa lesion, and the brain lesion was not confirmed pathologically. This case may represent brain invasion by inflammatory pseudotumor.

A common MR finding among our cases was hypointensity of the lesion on T2-weighted images. T2 hypointensity of a soft-tissue lesion is thought to be characteristic of fibrosing inflammatory pseudotumor. This hypointensity may be explained by a relative lack of both free water and mobile protons within fibrotic lesions. Diffuse fibrotic changes with various degrees of collagen deposition were seen at microscopic examination in all our cases. Calcification is a possible cause of T2 hypointensity of a lesion, but we saw no calcification on CT scans or histopathologic specimens.

On MR images, mobile protons are needed for enhancement of the lesion, and a fibrotic or hypercellular lesion enhances weakly. In one patient in our series (case 3), the lesion showed weaker enhancement on MR images than on CT scans, which can be explained by the densely fibrotic background of the lesion (Fig 2). There was no apparent difference in the contrast enhancement pattern on MR images and CT scans in the two other patients who were examined with both techniques.

It has been reported that high-grade malignant tumors of the parotid gland may appear hypointense on T2-weighted MR images (16). This signal characteristic presumably reflects the lack of serous and mucinous products, the high mitotic ratio, and the high nuclear-to-cytoplasmic ratios that are characteristic of high-grade malignant lesions of the parotid gland (16). If such a lesion were to occur at the skull base, it would be very difficult to distinguish from a lesion with fibrotic background, like those in our cases. Primary malignant tumors of the central skull base, such as chordomas or chondrosarcomas; direct invasion from nasopharyngeal carcinomas; and metastatic malignant tumors from distant primary sites are the most common malignant tumors of the skull base. The signal intensity of these lesions is usually isointense on T1-weighted images and isointense or slightly hyperintense on T2-weighted images.

Postinflammatory or postoperative fibrotic scars may also appear hypointense on T2-weighted images, but these entities usually do not show mass effects or bone destruction, and our patients had no history of surgery or specific inflammation of the head and neck.

Every patient in our series had signs or symptoms of various cranial nerve dysfunctions that were referable to MR findings. Ophthalmoplegia in two patients (cases 1 and 3) could be explained by the cavernous sinus involvement (Fig 2), trigeminal neuralgia (case 4) by an infiltration of the cranial base (Fig 1), facial palsy (case 2) by an involvement of the stylomastoid foramen (Fig 3), and hearing loss (case 5) by a thickening of the petroclival dura, including the internal auditory meatus. In every patient, treatment with oral corticosteroid therapy for more than a month after pathologic

diagnosis produced no objective improvement in cranial nerve dysfunction. We do not think that steroid therapy is helpful to improve dysfunction relating to long-standing fibrotic lesions such as these.

In summary, fibrotic inflammatory pseudotumor with involvement of the skull base may mimic malignant tumor with skull base invasion. MR imaging shows characteristic findings of infiltrative soft-tissue lesions, with bone destruction and hypointensity on T2-weighted images. A lack of mobile protons due to the densely fibrotic background of these lesions may account for this T2 hypointensity and weaker enhancement on MR images.

References

1. Chavis RM, Garner AG, Wright JE. Inflammatory orbital pseudotumors. *Arch Ophthalmol* 1978;96:1872–1922
2. Heersink B, Ridrigues MR, Flanagan JC. Inflammatory pseudotumor of the orbit. *Ann Ophthalmol* 1977;9:17–29
3. Som PM, Brandwein MS, Maldjian C, Reino AJ, Lawson W. Inflammatory pseudotumor of the maxillary sinus: CT and MR findings in six cases. *AJR Am J Roentgenol* 1994;163:689–692
4. Weisman RA, Osguthorpe JD. Pseudotumors of the head and neck masquerading as neoplasia. *Laryngoscope* 1988;98:610–614
5. Keen M, Conley J, McBride T, Mutter G, Silver J. Pseudotumor of the pterygomaxillary space presenting as anesthesia of the mandibular nerve. *Laryngoscope* 1986;96:560–563
6. Hytiroglou P, Brandwein MS, Strauchen JA, Mirante JP, Urken ML, Biller HF. Inflammatory pseudotumor of the parapharyngeal space: case report and review of the literature. *Head Neck* 1992; 14:230–234
7. Berardi RJ, Lee SS, Chen HP, Stines GJ. Inflammatory pseudotumors of the lungs. *Surg Gynecol Obstet* 1983;156:89–96
8. Eshaghian J, Anderson RL. Sinus involvement in inflammatory orbital pseudotumor. *Arch Ophthalmol* 1981;99:627–630
9. Blodi FC, Gass JD. Inflammatory pseudotumor of the orbit. *Trans Am Acad Ophthalmol Otolaryngol* 1967;71:303–323
10. Seider MJ, Cleary KR, van Tassel P, et al. Plasma cell granuloma of the nasal cavity treated by radiation therapy. *Cancer* 1991;67: 929–932
11. Tang TT, Segura AD, Oechler HW, et al. Inflammatory myofibrohistiocytic proliferation simulating sarcoma in children. *Cancer* 1990;65:1626–1634
12. West SG, Pittman DL, Coggin JT. Intracranial plasma cell granuloma. *Cancer* 1980;46:330–335
13. Curtin HD. Pseudotumor. *Radiol Clin North Am* 1987;25:583–599
14. Takimoto T, Kathoh T, Ohmura T, Kamide M, Nishimura T, Umeda R. Inflammatory pseudotumor of the maxillary sinus mimicking malignancy. *Rhinology* 1990;28:123–127
15. Garcia F de M, Aiguabella MAB, Liesa RF, Esteban JR, Aseno RMBY, Gonzalez EAV. Pseudotumor inflammatorio de senos paranasales. *Acta Otorrinolaringol Esp* 1990;41:351–353
16. Som PM, Biller HF. High-grade malignancies of the parotid gland: identification with MR imaging. *Radiology* 1989;173: 823–826